(DOI will not work until issue is live.) DOI: http://dx.doi.org/10.2138/am.2013.4496

Revision 1

Discovery of dmisteinbergite (hexagonal $CaAl_2Si_2O_8$) in the Allende meteorite: A new member of refractory silicates formed in the solar nebula

Chi Ma[1]*, Alexander N. Krot[2,3], and Martin Bizzarro[3]

[1]Division of Geological and Planetary Sciences, California Institute of Technology, Pasadena, California 91125, USA

[2]Hawai'i Institute of Geophysics and Planetology, University of Hawai'i at Manoa, Honolulu, Hawai'i 96822, USA

[3]Centre for Star and Planet Formation and Natural History Museum of Denmark, University of Copenhagen, DK-1350 Copenhagen, Denmark

ABSTRACT

Dmisteinbergite, $CaAl_2Si_2O_8$ with *P6₃/mcm* structure, was identified in a rounded coarse-grained igneous Type B2 Ca-,Al-rich inclusion (CAI) *STP-1* from the Allende CV3 carbonaceous chondrite. *STP-1* belongs to a very rare type of refractory inclusions, FUN (Fractionation and Unknown Nuclear effects) CAIs, which experienced melt evaporation and crystallization at low total gas pressure (P < 10^{-6} bar) in a high-temperature (> 1200°C) region, possibly near the proto-Sun and were subsequently radially transported away from region, possibly by a disk wind. The Allende dmisteinbergite occurs as irregular single crystals (100–600 µm in size) in contact with gehlenitic melilite and Al,Ti-diopside, poikilitically enclosing euhedral spinel, and rare anorthite. It is colorless and transparent. The mean chemical composition, determined by electron microprobe analysis, is (wt%) SiO_2 42.6, Al_2O_3 36.9, CaO 20.2, MgO 0.05, sum 99.75, giving rise to an empirical formula of $Ca_{1.01}Al_{1.96}Si_{2.02}O_8$. Its electron backscatter diffraction patterns are a good match to that of synthetic $CaAl_2Si_2O_8$ with the $P6_3/mcm$ structure and the unit cell a = 5.10 Å, c = 14.72 Å, and Z = 2. Dmisteinbergite could have crystallized from a silicate melt at high temperature (~1200–1400°C) via rapid cooling. Dmisteinbergite in Allende, the first find in a meteorite, is a new member of refractory silicates, among the first solid materials formed in the solar nebula.

Keywords: dmisteinbergite, hexagonal $CaAl_2Si_2O_8$, new refractory silicate, Allende meteorite, carbonaceous chondrite, Ca-, Al-rich refractory inclusion, solar nebula, EBSD

----

*E-mail: chi@gps.caltech.edu

INTRODUCTION

We identified dmisteinbergite, $CaAl_2Si_2O_8$ with *P6₃/mcm* structure, in the recently discovered coarse-grained, igneous Type B2 FUN (Fractionation and Unknown Nuclear effects) Ca,Al-rich refractory inclusion (CAI), named *STP-1*, from the Allende meteorite (Holst et al. 2012). The Allende meteorite, which fell at Pueblito de Allende, Chihuahua, Mexico on February 8, 1969, is a CV3 carbonaceous chondrite, which contains refractory inclusions, chondrules and matrix binding the rock together. The Allende meteorite is often considered the best-studied meteorite. Current understanding on the early solar evolution is largely based on intensive studies of components in this meteorite. Refractory inclusions are among the oldest solid objects formed in the solar system. Each and every new refractory phase reveals distinctive forming conditions, providing new insight into solar nebula processes.

Dmisteinbergite was previously only found in burned coal dumps from Chelyabinsk Coal Basin, Ural Mountains, Russia (Chesnokov et al. 1990), and in a pseudotachylite from the Gole Larghe Fault, Adamello batholith, Italy (Nestola et al. 2010), formed at high temperatures. Unpublished data on-line at webmineral.com and mindat.org also describe low temperature hydrothermal dmisteinbergite in Kurumazawa gabbro quarry, Katashina, Gumma, Japan. Synthetic hexagonal $CaAl_2Si_2O_8$ is well studied (e.g., Takeuchi and Donnay 1959; Abe et al. 1991; Borghum et al. 1993; Abe and Sunagawa 1995). We report here the first occurrence of dmisteinbergite in a meteorite as a new refractory mineral in a CAI and consider its origin and implication for the formation of *STP-1*. Dmisteinbergite is one of nine refractory silicates identified in refractory inclusions to date.

Dmisteinbergite (hexagonal), svyatoslavite (monoclinic), and anorthite (triclinic) are polymorphs of $CaAl_2Si_2O_8$. Dmisteinbergite has a layered structure, stacking double sheets of 6-membered rings of $(Si,Al)O_4$ tetrahedra with Ca in between layers (Takeuchi and Donnay 1959). Svyatoslavite displays a pseudo-orthorhombic three-dimensional network of SiO_4 and AlO_4 tetrahedra with Ca at the interstitial sites (Krivovichev et al. 2012). Anorthite has a more complex structure.

EXPERIMENTAL

Electron probe microanalysis (EPMA), scanning electron microscopy (SEM) in backscatter electrons (BSE), and electron backscatter diffraction (EBSD) were used to characterize chemical composition and structure of dmisteinbergite and associated phases. A JEOL JXA-8500F field emission EPMA was operated at 15 kV, 20 nA for back-scatter electron imaging, x-ray mapping and quantitative elemental analysis.

Crystal structure study by EBSD at a sub-micrometer scale was carried out using methods described in Ma and Rossman (2008, 2009a) with an HKL EBSD system on a ZEISS 1550VP scanning electron microscope operated at 20 kV and 6 nA in a focused beam with a 70° tilted stage and in a variable pressure mode (25 Pa). The structure was determined and cell constants obtained by testing the experimental EBSD pattern against the structures of synthetic hexagonal $CaAl_2Si_2O_8$ (Takeuchi and Donnay 1959; Dimitrijevic et al. 1996), anorthite (Angel et al. 1990), svyatoslavite (Takeuchi et al. 1973; Krivovichev et al. 2012), celsian (Griffen and Ribbe 1976) and paracelsian (Chiari et al. 1985).

RESULTS

Mineralogy and petrology of the host CAI

STP-1 is a coarse-grained igneous Type B2 (without melilite mantle) CAI composed of pure $CaAl_2Si_2O_8$ (mostly dmisteinbergite and rare anorthite), gehlenitic melilite ($Åk_{6–28}$), and igneously-zoned Al,Ti-diopside (Al_2O_3 = 17.7−28.5 wt.%, TiO_2 = 0.03−8.7 wt.%), all poikilitically enclosing euhedral compositionally near pure spinel grains (Figs. 1, 2). Lath-shaped hibonite grains and spinel-hibonite intergrowths occur in the outermost portion of the inclusion (Fig. 2d). The hibonite grains have low contents of MgO (0.2−1.7 wt.%) and TiO_2 (0.09−3.2 wt.%). No multilayered Wark-Lovering rim sequence is observed around *STP-1*. The CAI experienced only a small degree of secondary alteration resulted in replacement of melilite by nepheline, sodalite, Fe-bearing Al-rich, Ti-poor pyroxene (FeO, 2.5−6.3 wt.%, Al_2O_3, 5.1−16.2 wt.%, TiO_2, 0.10−0.27 wt.%), and Na-bearing plagioclase (0.35−0.89 wt.% Na_2O), and enrichment of spinel in FeO (up to 19.5 wt.%) in its peripheral portion (Figs. 1a,c,d). In addition, melilite crystals are crosscut by thin veins of grossular, Al-diopside, and Na-bearing plagioclase (Fig. 2).

Appearance, chemistry and crystallography of dmisteinbergite

Dmisteinbergite occurs as irregular single crystals (100–600 µm in size, as revealed by EBSD analysis) with perfect cleavage {001} lines on the section plane (Fig. 2). Euhedral anorthite inclusions are observed inside one of the dmisteinbergite crystals (Fig. 2d), where anorthite appears to have a higher BSE albedo than dmisteinbergite likely due to electron channeling effects. Dmisteinbergite and anorthite show no evidence for replacement by secondary minerals. Some of the cleavage planes in dmisteinbergite, however, are filled by secondary grossular (Figs. 2b,d).

Dmisteinbergite is colorless and transparent. Its chemical composition is given in Table 1, showing empirical formula of $Ca_{1.01}Al_{1.96}Si_{2.02}O_8$. One dmisteinbergite grain has two Ba-rich domains (Fig. 2c) with an empirical formula of $(Ca_{0.74}Ba_{0.27})Al_{1.93}Si_{2.05}O_8$ (Table 1). The dmisteinbergite grain and the two Ba-rich domains have the same crystal orientation, as revealed by EBSD analysis.

EBSD patterns of dmisteinbergite and Ba-rich dmisteinbergite were obtained, which can only be indexed using the hexagonal $P6_3/mcm$ $CaAl_2Si_2O_8$ structure and this yields the best fit based on synthetic $CaAl_2Si_2O_8$ from Takeuchi and Donnay (1959) (Figs. 3,4) with the unit cell a = 5.10 Å, c = 14.72 Å, V = 331.57 Å^3 and Z = 2. Anorthite included in dmisteinbergite (Fig. 2d), was also identified by EBSD, as shown in Fig. 5.

DISCUSSION

STP-1 belongs to a very rare type of refractory inclusions, FUN (Fractionation and Unknown Nuclear effects) CAIs (e.g., Wasserburg et al. 1977), which may have experienced melt evaporation and crystallization at low total gas pressure (P < 10^{-6} bar) in a high-temperature (> 1200°C) region (e.g., Mendybaev et al. 2009), possibly near the proto-Sun, and were subsequently radially transported away from region by some mechanism, e.g., by disk wind (Shu et al. 1996) or by turbulent diffusion (Yang and Ciesla 2012). Coarse-grained dmisteinbergite in *STP-1* is apparently not produced by hydrothermal process. It is most likely crystallized metastably from a silicate melt at high temperature (~1200−1400°C) via rapid cooling, as indicated by study of synthesizing hexagonal $CaAl_2Si_2O_8$ from melt (Abe et al. 1991). Ba-bearing dmisteinbergite may be also igneous in origin. Prior to its crystallization, the melt experienced evaporation at low total pressure that resulted in mass-dependent fractionation of oxygen and magnesium isotopes (Holst et al. 2012). The presence of coarse euhedral anorthite inclusions in one of the dmisteinbergite grains (Fig. 2) may reflect either primary, igneous origin of anorthite or post-crystallization transformation of metastable dmisteinbergite to anorthite during subsequent reheating. Crystallization of anorthite prior to dmisteinbergite from the host CAI melt is inconsistent with anorthite melt experiments of Abe et al. (1991) and abundant pores observed within anorthite (Fig. 2), which might have resulted from volume change during transformation of dmisteinbergite to anorthite. The late-stage crystallization of anorthite will be tested by oxygen and magnesium-isotope measurements of anorthite and dmisteinbergite; this work is in progress. Although there are no indications that the anorthite now in normal (non-FUN) CAIs was once dmisteinbergite, identification of anorthite in CAIs should be re-examined, and confirmed by EBSD when possible. A simple approach to distinguish the two is to check cleavage lines on section planes. Dmisteinbergite shows one set of perfect cleavages whereas anorthite displays no cleavages. The CAI *STP-1* experienced relatively minor secondary alteration on the Allende parent asteroid that resulted in formation of grossular, Al-diopside, Na-bearing plagioclase, nepheline, and sodalite.

Dmisteinbergite is a new member of refractory silicates, joining other eight refractory silicates melilite, Al,Ti-diopside, anorthite, and newly-approved davisite $Ca(Sc,Mg,Ti^{3+},Ti^{4+})AlSiO_6$ (Ma and Rossman 2009b), grossmanite $Ca(Ti^{3+},Mg,Ti^{4+})AlSiO_6$ (Ma and Rossman 2009c), kushiroite $CaAlAlSiO_6$ (Kimura et al. 2009; Ma et al. 2009), and newly-identified eringaite $Ca_3(Sc,Y,Ti)_2Si_3O_{12}$ (Ma 2012), and thortveitite $Sc_2Si_2O_7$ (Ma et al. 2011), among the oldest solid materials formed in the solar system. Thortveitite, eringaite, and davisite are ultrarefractory silicates, formed earlier in the solar nebula before the occurrence of melilite and dmisteinbergite, followed by Al,Ti-diopside, anorthite, grossmanite, and kushiroite.

ACKNOWLEDGEMENTS

SEM-EBSD was carried out at the Geological and Planetary Science Division Analytical Facility, Caltech, which is supported in part by NSF EAR-0318518 and DMR-0080065. This work was also supported by NASA grant NNX12AJ01G (ANK, PI). We would like to thank Andrew M. Davis, Alan Rubin, Péter Németh, an anonymous reviewer and editor Ian Swainson for helpful comments and suggestions.

REFERENCES

Abe, T. and Sunagawa, I. (1995) Hexagonal $CaAl_2Si_2O_8$ in a high-temperature solution; metastable crystallization and transformation to anorthite. Mineralogical Journal, 17, 257–281.

Abe, T., Tsukamoto, K., and Sunagawa, I. (1991) Nucleation, growth and stability of $CaAl_2Si_2O_8$ polymorphs. Physics and Chemistry of Minerals, 17, 473–484.

Angel, R.J., Carpenter, M.A., and Finger, L.W. (1990) Structural variation associated with compositional variation and order-disorder behavior in anorthite-rich feldspars. American Mineralogist, 75, 150–162.

Borghum, B.P., Bukowski, J.M., and Young, J.F. (1993) Low-temperature synthesis of hexagonal anorthite via hydrothermal processing. Journal of the American Ceramic Society, 76, 1354–1356.

Chesnokov, B.V., Lotova, E.V., Nigmatulina, E.N., Pavlyuchenko, V.S., and Bushmakin, A.F. (1990) Dmisteinbergite $CaAl_2Si_2O_8$ (hexagonal) – A new mineral. Zapiski Vsesoyuz Mineralogicheskogo Obshchestva, 119, 43–45.

Chiari, G., Gazzoni, G., Craig, J.R., Gibbs, G.V., and Louisnathan, S.J. (1985) Two independent refinements of the structure of paracelsian, $BaAl_2Si_2O_8$. American Mineralogist, 70, 969–974.

Dimitrijevic, R., Dondur, V., and Kremenovic, A. (1996) Thermally induced phase transformations of Ca-exchanged LTA and FAU zeolite frameworks: Rietveld refinement of the hexagonal $CaAl_2Si_2O_8$ diphyllosilicate structure. Zeolites, 16, 294–300.

Griffen, D.T. and Ribbe, P.H. (1976) Refinement of the crystal structure of celsian. American Mineralogist, 61, 414–418.

Holst, J.C., Olsen, M.B., Wielandt, D., Paton, C., and Bizzarro, M. (2012) Towards a ^{182}Hf-^{182}W chronology of FUN CAIs. Meteoritics & Planetary Science, 47 (S1), A190.

Kimura, M., Mikouchi, T., Suzuki, A., Miyahara, M., Ohtani, E., and El Goresy, A. (2009) Kushiroite, $CaAlAlSiO_6$: A new mineral of the pyroxene group from the ALH 85085 CH chondrite, and its genetic significance in refractory inclusions. American Mineralogist, 94, 1479-1482.

Krivovichev, S.V., Shcherbakova, E.P., and Nishanbaev, T.P. (2012) The crystal structure of svyatoslavite and evolution of complexity during crystallization of a $CaAl_2Si_2O_8$ melt: A structural automata description. The Canadian Mineralogist, 50, 585–592.

Ma, C. (2012) Discovery of meteoritic eringaite, $Ca_3(Sc,Y,Ti)_2Si_3O_{12}$, the first solar garnet? Meteoritics & Planetary Science, 47 (S1), A256.

Ma, C. and Rossman, G.R. (2008) Barioperovskite, $BaTiO_3$, a new mineral from the Benitoite Mine, California. American Mineralogist, 93, 154−157.

Ma, C. and Rossman, G.R. (2009a) Tistarite, Ti_2O_3, a new refractory mineral from the Allende meteorite. American Mineralogist, 94, 841−844.

Ma, C. and Rossman, G.R. (2009b) Davisite, $CaScAlSiO_6$, a new pyroxene from the Allende meteorite. American Mineralogist, 94, 845−848.

Ma, C. and Rossman, G.R. (2009c) Grossmanite, $CaTi^{3+}AlSiO_6$, a new pyroxene from the Allende meteorite. American Mineralogist, 94, 1491−1494.

Ma, C., Simon, S.B., Rossman, G.R., and Grossman, L. (2009) Calcium Tschermak's pyroxene, $CaAlAlSiO_6$, from the Allende and Murray meteorites: EBSD and micro-Raman characterizations. American Mineralogist, 94, 1483−1486.

Ma, C., Beckett, J.R., Tschauner, O., and Rossman, G.R. (2011) Thortveitite ($Sc_2Si_2O_7$), the first solar silicate? Meteoritics & Planetary Science, 46 (S1), A144.

Mendybaev, R.A., Richter, F.M., Georg, R.B., and Davis, A.M. (2009) Evaporation kinetics of forsterite-rich melts and thermal histories of FUN CAIs. 40th Lunar and Planetary Science Conference, Abstract # 2461.

Nestola, F., Mittempergher, S., Di Toro, G., Zorzi, F., and Pedron, D. (2010) Evidence of dmisteinbergite (hexagonal form of $CaAl_2Si_2O_8$) in pseudotachylyte: A tool to constrain the thermal history of a seismic event. American Mineralogist, 95, 405–409.

Shu, F.H., Shang, H., and Lee, T. 1996. Toward an astrophysical theory of chondrites. Science, 271, 1545−1552.

Takeuchi, Y. and Donnay, G. (1959) The crystal structure of hexagonal $CaAl_2Si_2O_8$. Acta Crystallographica, 12, 465–470.

Takeuchi, Y., Haga, N., and Ito, J. (1973) The crystal structure of monoclinic $CaAl_2Si_2O_8$: a case of monoclinic structure closely simulating orthorhombic symmetry. Zeitschrift fur Kristallographie, 137, 380–398.

Wasserburg, G.J., Lee, T., and Papanastassiou, D.A. (1977) Correlated O and Mg isotopic anomalies in Allende inclusions. II – Magnesium. Geophysical Research Letters, 4, 299–302.

Yang, L. and Ciesla, F.J. (2012) The effects of disk building on the distributions of refractory materials in the solar nebula. Meteoritics & Planetary Science, 47, 99–119.

This is a preprint, the final version is subject to change, of the American Mineralogist (MSA)
Cite as Authors (Year) Title. American Mineralogist, in press.
(DOI will not work until issue is live.) DOI: http://dx.doi.org/10.2138/am.2013.4496 7/11

Table 1. Mean elemental composition of dmisteinbergite and Ba-rich dmisteinbergite in the Allende CAI.

	Dmisteinbergite	Ba-rich dmisteinbergite
Constituent	wt%	wt%
SiO_2	42.6(3)[a]	38.18(2)
Al_2O_3	36.9(3)	35.6(4)
CaO	20.2(1)	13.45(4)
MgO	0.05(6)	0.16(5)
BaO	n.d.[b]	11.7(4)
Na_2O	b.d.[c]	0.20(2)
Total	99.75	99.29

[a]Errors given inside parentheses are one standard deviation of the mean based on all of the analyses.

[b]n.d.: not determined.

[c]b.d.: below dection limit, Na 0.03 wt%.

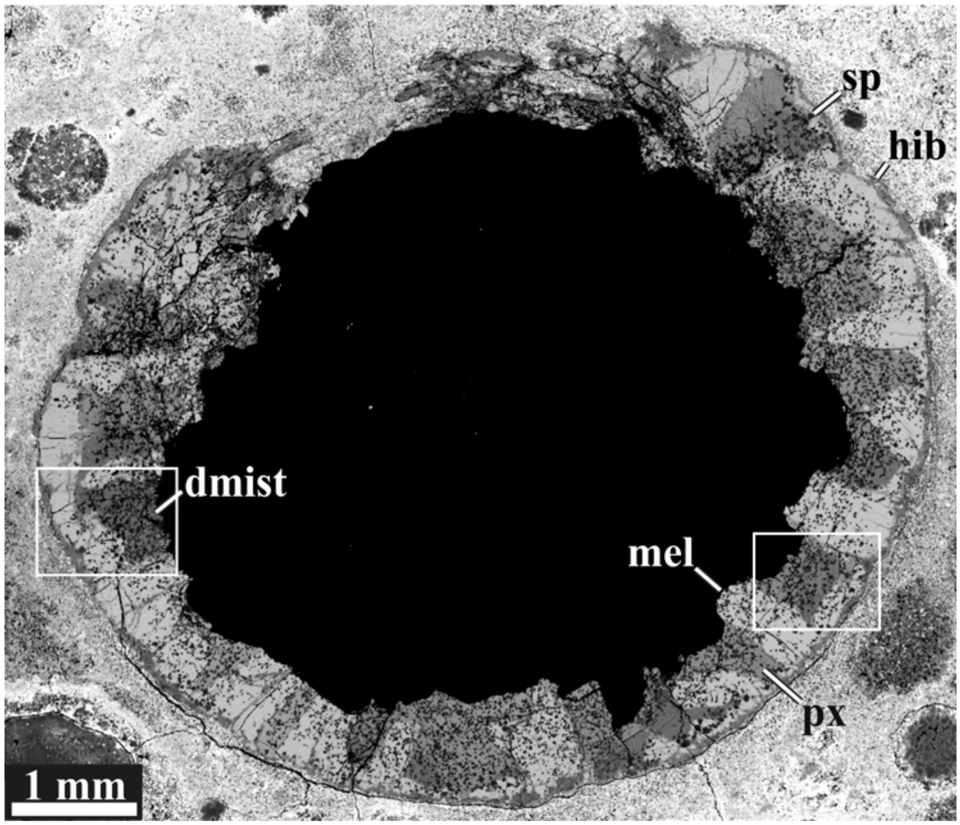

Fig. 1. Backscatter electron image of the Allende FUN Type B2 CAI *STP-1*. The central part of the CAI was lost during sample preparation. Regions outlined are shown in Fig. 2. The CAI consists of melilite, igneously-zoned A,Ti-diopside, and dmisteinbergite, all poikilitically enclosing euhedral spinel grains. Hibonite intergrown with spinel occurs in the outermost region of *STP-1*. The CAI experienced relatively minor secondary alteration resulted in formation of Na-rich minerals (nepheline and sodalite) in the peripheral zone and of grossular-rich veins crosscutting melilite. px = aluminum-titanium diopside; dmist = dmisteinbergite; hib = hibonite; mel = melilite; sp =spinel.

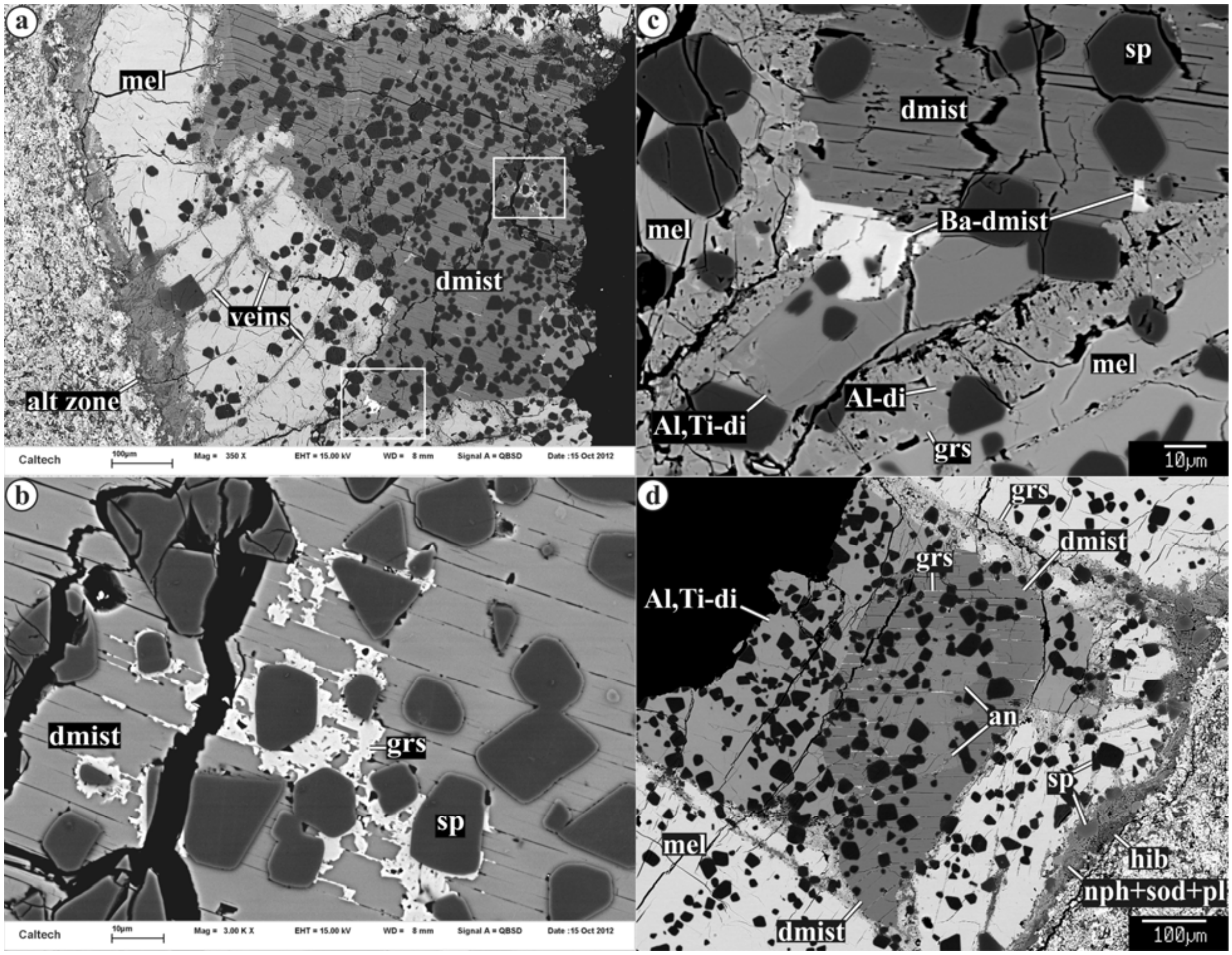

Fig. 2. Backscatter electron images illustrating primary and secondary mineralogy of *STP-1* and occurrences of dmisteinbergite. Regions outlined in “a” are shown in detail in “b” and “c”. a – Melilite in the outermost region of the CAI is replaced by nepheline, sodalite, and Na-bearing plagioclase and crosscut by grossular-rich veins. c – The coexisting Ba-rich dmisteinbergite, dmisteinbergite, melilite, spinel, and Al,Ti-diopside. Melilite is partly replaced by grossular and Ti-free Al-diopside. d – Dmisteinbergite enclosing anorthite; some cleavage planes in dmisteinbergite are filled by secondary grossular. Al-di = aluminum diopside; Al,Ti-di = aluminum-titanium diopside; alt = alteration; an = anorthite; Ba-dmist = barium dmisteinbergite; dmist = dmisteinbergite; grs = grossular; hib = hibonite; mel = melilite; nph = nepheline; pl = sodium-bearing plagioclase; sod = sodalite; sp =spinel.

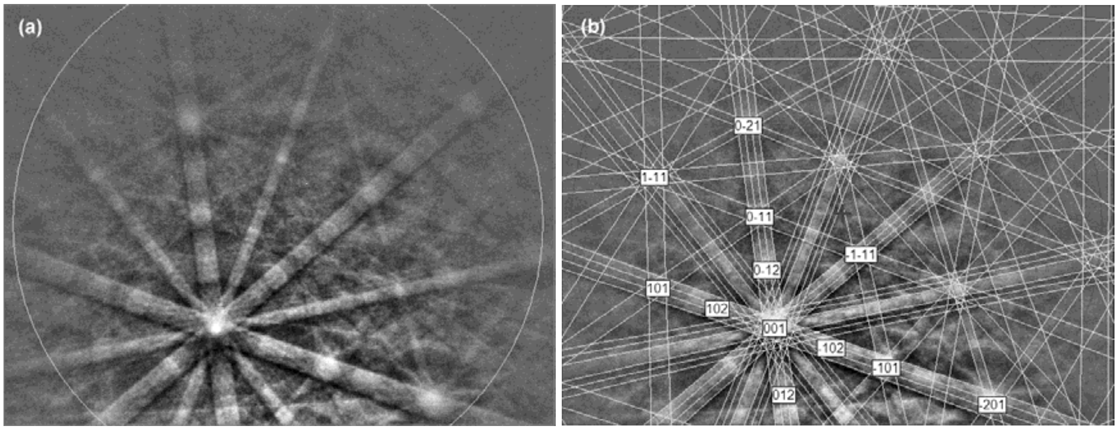

Fig. 3. a – EBSD pattern of the dmisteinbergite crystal in Fig. 2d. b – Pattern indexed with the *P6₃/mcm* synthetic $CaAl_2Si_2O_8$ structure.

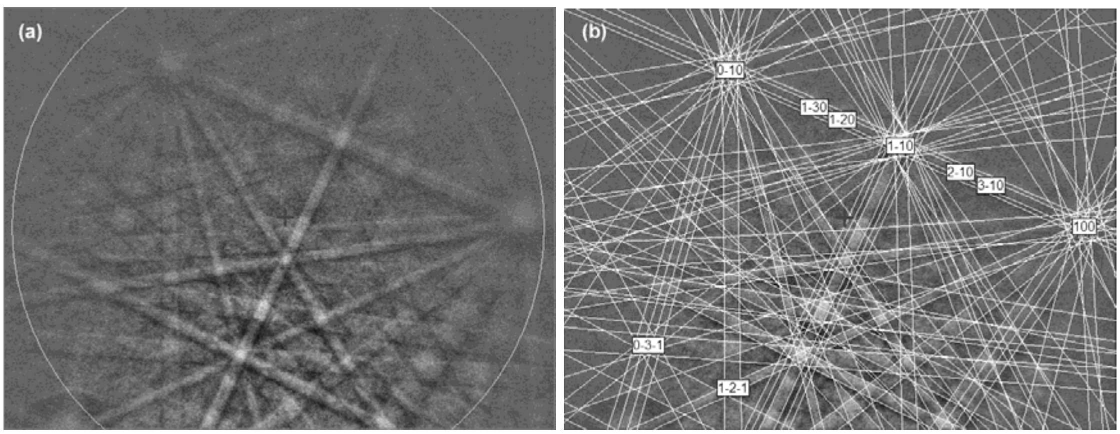

Fig. 4. a – EBSD pattern of the Ba-rich dmisteinbergite crystal in Fig. 2c. b – Pattern indexed with the *P6₃/mcm* synthetic $CaAl_2Si_2O_8$ structure.

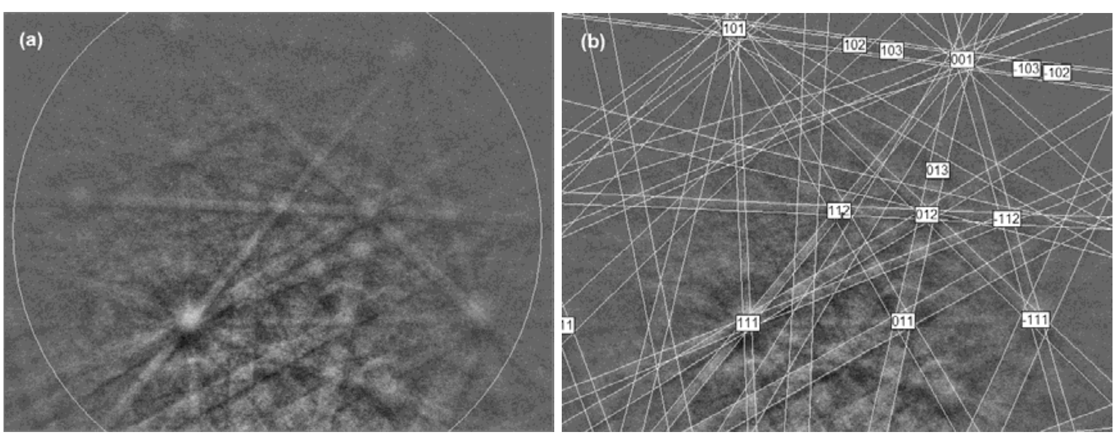

Fig. 5. a – EBSD pattern of the anorthite crystal in Fig. 2d. b – Pattern indexed with the *P-1* anorthite structure.